Orbital-dependent polaron formation in the relativistic Mott insulator Sr$_2$IrO$_4$

C. H. Sohn,[1,2] Min-Cheol Lee,[1,2] H. J. Park,[1,2] Kyung Joo Noh,[1] H. K. Yoo,[1,2] S. J. Moon,[3] K. W. Kim,[4] T. F. Qi,[5] G. Cao,[5]
Deok-Yong Cho,[1,2,6,*] and T. W. Noh[1,2,†]

[1]*Center for Correlated Electron Systems, Institute for Basic Science, Seoul National University, Seoul 151-747, Korea*
[2]*Department of Physics and Astronomy, Seoul National University, Seoul 151-747, Korea*
[3]*Department of Physics, Hanyang University, Seoul 133-791, Korea*
[4]*Department of Physics, Chungbuk National University, Cheong-ju, Chungbuk 361-763, Korea*
[5]*Center for Advanced Materials, Department of Physics and Astronomy, University of Kentucky, Lexington, Kentucky 40506, USA*
[6]*Department of Physics, Chonbuk National University, Jeonju 561-756, Korea*

We use optical spectroscopy to investigate the electron-phonon interaction in Sr$_2$IrO$_4$, a well-known $5d$ transition metal oxide with spin-orbit entangled states. The temperature evolution in the optical spectra is well described by the Fröhlich polaron model, indicating a large electron-phonon interaction. We further find that electrons in different orbitals selectively couple with different phonon modes. While $J_{\text{eff}} = 3/2$ holes do not seem to couple with any phonons, $J_{\text{eff}} = 1/2$ and $3z^2$-r^2 electrons mainly couple with in-plane and out-of-plane Ir-O bending modes, respectively. The symmetries of the orbitals and phonons are consistent with our observations.

Recently, $5d$ transition metal oxides (TMOs) have been attracting rising interest because the underlying physics in these systems is different from that in $3d$ TMOs. Compared to $3d$ TMOs, $5d$ TMOs are characterized by an enhanced single-electron bandwidth, reduced Coulomb interaction, and large spin-orbit coupling (SOC). Thus, the electronic structures of $5d$ TMOs should be determined by cooperation and/or competition among three energy scales, and the resulting ground states may be fundamentally different from those of $3d$ TMOs. Indeed, it has been shown and proposed that $5d$ TMOs have a variety of exotic phases, including a relativistic Mott insulator [1–3], a correlated topological insulator [4–6], and a quantum spin liquid [7–11]. These novel ground states in $5d$ TMOs are born from the effective total angular momentum ($J_{\text{eff}} = L_{\text{eff}} + S$) states induced by strong SOC [1,2], where the spin and orbital degrees of freedom are naturally entangled.

Despite the great interest in $5d$ TMOs, it remains unclear how and if electrons in J_{eff} states couple with other degrees of freedom, such as phonons. Electron-phonon (e-ph) interactions in $3d$ TMOs have been extensively studied in a number of experiments [12–16], because they dominate the low-energy physics of electrons by renormalizing the mass of charge carriers. Likewise, in the case of $5d$ TMOs, strong e-ph interactions have been suggested by a couple of recent experimental studies for Sr$_3$Ir$_2$O$_7$ [17,18], Na$_2$IrO$_3$ [19], and Na$_3$Ir$_3$O$_8$ [20]. Since orbitals of $5d$ electrons are larger than those of $3d$ electrons, e-ph interactions could be more important in $5d$ TMOs. Therefore, detailed and quantitative studies on the e-ph interaction in $5d$ TMOs are required not only for a deeper understanding of those systems, but also for exploring novel phenomena, including superconductivity.

Here, we present a clear signature of an orbital-dependent e-ph interaction in Sr$_2$IrO$_4$, a representative $5d$ TMO, by means of optical spectroscopy. This material is the most well-known relativistic Mott insulator driven by strong SOC [1,2]. We

find that the energies of d-d transitions, even up to 3 eV, show strong and systematic redshifts with increasing temperature (T). By analyzing the peak shifts of d-d transitions, we could extract the self-energies of the electrons and holes. The T dependences of the self-energies are well explained by adopting the Fröhlich polaron model [21,22], indicating the existence of large e-ph interactions. Furthermore, we show that the e-ph interaction in Sr$_2$IrO$_4$ varies depending on the orbital symmetries. Namely, $J_{\text{eff}} = 1/2$ electrons and holes ($3z^2$-r^2 electrons) effectively couple with 54 meV (32 meV) phonon mode, whereas $J_{\text{eff}} = 3/2$ holes do not couple with any phonons. Considering the symmetries of the orbitals and phonons, we propose that in-plane and out-of-plane bending modes in the local Ir-O octahedron mainly couple with $J_{\text{eff}} = 1/2$ and $3z^2$-r^2 electrons, respectively.

A high-quality single crystal of Sr$_2$IrO$_4$ was grown using a self-flux method [23]. After cleaving the sample to obtain a clean surface, we measured the near-normal reflectance of Sr$_2$IrO$_4$ between 10 meV and 1.0 eV by using a Fourier-transform infrared spectrometer. The values of reflectance were normalized by those measured after *in situ* gold evaporation for compensating the effect of rough surfaces [24]. We directly obtained dielectric constants [$\varepsilon(\omega) = \varepsilon_1(\omega) + i\varepsilon_2(\omega)$] for the higher-energy region (between 0.74 and 4.0 eV) using a V-VASE ellipsometer (J. A. Woollam Co.). Then we performed the Kramers-Kronig analysis to obtain dielectric constants below 0.74 eV. The real part of the optical conductivity $\sigma_1(\omega) = \omega\varepsilon_2(\omega)/4\pi$ and the energy-loss function $-\text{Im}[1/\varepsilon(\omega)]$ are calculated to examine the transverse and longitudinal optical (LO) excitations.

Figure 1(a) shows $\sigma_1(\omega)$ measured at various T from 25 to 400 K. With a broad spectral weight from the p-d transition (dashed line) [25], we found five distinct features below 4.0 eV, as indicated by α, β, γ, A, and B, in order of increasing photon energy. Based on previous photoemission [1] and x-ray absorption spectroscopy (XAS) [25] studies, we assigned the five peaks in $\sigma_1(\omega)$ as d-d transitions. It is well known that in Sr$_2$IrO$_4$, strong SOC transforms t_{2g} orbitals into $J_{\text{eff}} = 1/2$ and 3/2 (spin-entangled) orbital states. Then, electron correlation

---

*Email address: zax@jbnu.ac.kr
†Email address: twnoh@snu.ac.kr
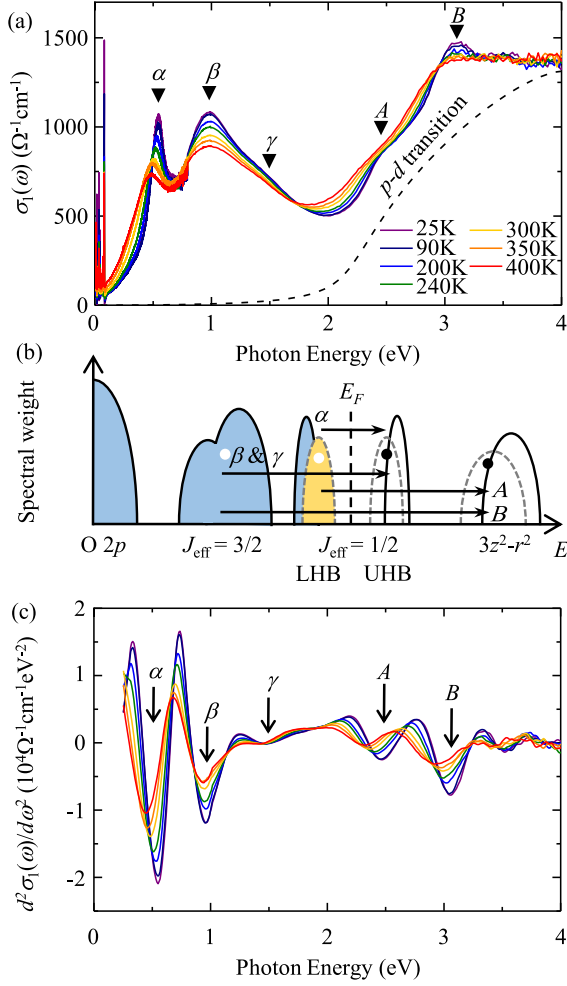
FIG. 1. (Color online) (a) T-dependent $\sigma_1(\omega)$ of Sr_2IrO_4. The black dashed line indicates the contribution of broad p-d transitions. Five sharp electronic transitions are indicated by α, β, γ, A, and B, in order of increasing energy. (b) Schematic diagram of the optical transition and spectral weights in Sr_2IrO_4. The solid (dashed) line represents the spectral weights in a noninteracting (interacting) system. (c) Second derivatives of $\sigma_1(\omega)$, $d^2\sigma_1(\omega)/d\omega^2$. The black arrows indicate the dips in $d^2\sigma_1(\omega)/d\omega^2$, corresponding to the peak energies in $\sigma_1(\omega)$.

further splits $J_{eff} = 1/2$ states into upper and lower Hubbard bands (UHB and LHB), resulting in a relativistic Mott insulator [1,2]. Therefore, we assigned the peak α (peaks β and γ) as the d-d transition from $J_{eff} = 1/2$ LHB ($J_{eff} = 3/2$) to $J_{eff} = 1/2$ UHB.

The unoccupied e_g state is located above the UHB. A previous O K-edge XAS study revealed that the lowest unoccupied e_g subband is more concentrated along the z direction [25], suggesting that it is mainly composed of the $3z^2$-r^2 orbital. Thus, we assigned peak A (B) as the transition from the $J_{eff} = 1/2$ LHB ($J_{eff} = 3/2$) to the unoccupied $3z^2$-r^2 orbital. The black solid lines and arrows in Fig. 1(b) schematically show the density of the states and optical transitions in Sr_2IrO_4, respectively. The dashed lines, which will be discussed later, indicate the T evolution of the spectral weights of the electrons and holes.
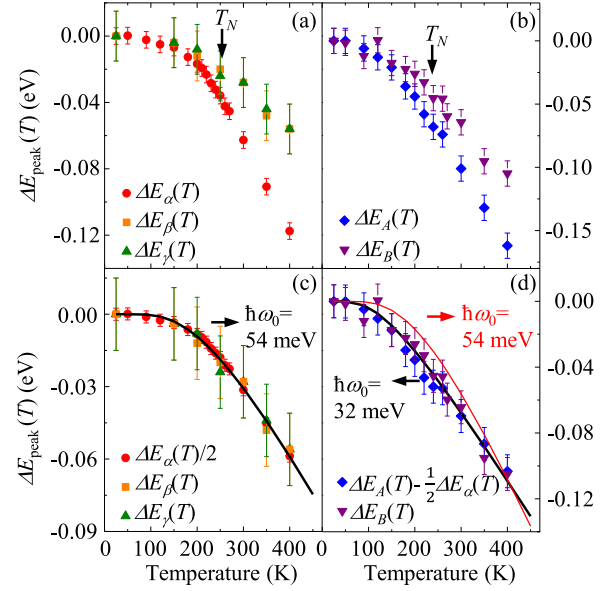
FIG. 2. (Color online) $\Delta E_{peak}(T)$ for (a) peaks α, β, and γ, and (b) peaks A and B. (c) $\Delta E_\alpha(T)/2$, $\Delta E_\beta(T)$, and $\Delta E_\gamma(T)$, which represent $\Sigma'(T)$ of $J_{eff} = 1/2$ electrons. The black thick line is the best fitting result with the Fröhlich polaron model. (d) $\Delta E_A(T) - \Delta E_\alpha(T)/2$ and $\Delta E_B(T)$, which represent $\Sigma'(T)$ of $3z^2$-r^2 electrons. The black thick line is the best fitting result with the polaron model, while the red thin line is the fitting line with 54 meV phonon energy for comparison.

All of the features of d-d transitions in Fig. 1(a) show a significant redshift with increasing T. This redshift is most pronounced in peak α, which has a narrow bandwidth. To investigate these spectral shifts more clearly, we plotted the second derivative of the spectra $d^2\sigma_1(\omega)/d\omega^2$ in Fig. 1(c). The dips in $d^2\sigma_1(\omega)/d\omega^2$, indicated by the arrows, correspond to the peaks in $\sigma_1(\omega)$. For peak α, the energy difference between 25 and 400 K data is ~0.12 eV, the magnitude of which far exceeds the thermal energy scale (~0.03 eV). For peaks β and γ, the corresponding energy difference is ~0.06 eV, which is roughly half of that of peak α. For peaks A and B, the corresponding energy differences are ~0.16 and ~0.11 eV, respectively.

The energy shifts of the d-d transitions in $\sigma_1(\omega)$ cannot be explained by the Slater mechanism, the Mott mechanism, or thermal expansion. We plotted $\Delta E_{peak}(T)$, the relative peak energies from $T = 25$ K data, for the five d-d transitions in Figs. 2(a) and 2(b) [26]. The energies of all five peaks show qualitatively similar T dependences, implying that such spectral changes share a single origin. Coupling with magnetic ordering might be one possible origin, but these peak shifts are rather gradual in T, without any clear anomaly near the antiferromagnetic ordering temperature $T_N \sim 240$ K. This suggests that the T evolution of $\sigma_1(\omega)$ is not dominated by the magnetic transition. The large changes even in the high-energy region (peaks A and B) seem to be related to the Mott mechanism. However, the Mott transition should undergo a first-order structural phase transition, which is inconsistent with our observations. Previous studies [27] reported that the T dependence of the unit cell volume at temperatures between 10 and 300 K is not significant ($\sim0.5\%$), implying that the

peak shifts observed here can hardly be dominated by certain thermal expansions.

Because there is no suitable reason for bare electronic structures to change with T, we propose that the energy shifts of d-d transitions originate from the T evolution of the self-energies induced by many body interactions. To obtain further insight into the origin of the peak shifts, we extracted the real part of the self-energies $\Sigma'(T)$ of the $J_{\rm eff} = 1/2$ and $3/2$ electrons from $\Delta E_\alpha(T)$, $\Delta E_\beta(T)$, and $\Delta E_\gamma(T)$. Because optical transitions always generate electrons and holes in pairs, the $\Sigma'(T)$'s of both the electrons and holes contribute to the peak shifts. For peak α, we could assume that the $\Sigma'(T)$'s are the same for the electrons and holes because they occupy the same $J_{\rm eff} = 1/2$ orbitals. Therefore, $\Delta E_\alpha(T)/2$ plotted in Fig. 2(c) indicates the $\Sigma'(T)$ of $J_{\rm eff} = 1/2$ electrons. Interestingly, $\Delta E_\alpha(T)/2$ is similar to $\Delta E_\beta(T)$ and $\Delta E_\gamma(T)$ across a wide range of T. It should be noted that peaks β and γ generate electrons and holes in the $J_{\rm eff} = 1/2$ and $J_{\rm eff} = 3/2$ orbitals, respectively. Therefore, the similar T dependences of $\Delta E_\alpha(T)/2$, $\Delta E_\beta(T)$, and $\Delta E_\gamma(T)$ in Fig. 2(c) suggest that the $\Sigma'(T)$'s of the $J_{\rm eff} = 3/2$ holes are nearly T independent, and only the $\Sigma'(T)$'s of the excited electrons in $J_{\rm eff} = 1/2$ UHB contribute to the redshift of peaks β and γ.

Likewise, the $\Sigma'(T)$'s of $3z^2$-r^2 electrons can be deduced either from $\Delta E_A(T)$ or $\Delta E_B(T)$. Because transition A generates $J_{\rm eff} = 1/2$ holes and $3z^2$-r^2 electrons, $\Delta E_A(T)$ is the sum of their $\Sigma'(T)$ values. Since $\Sigma'(T)$ of the $J_{\rm eff} = 1/2$ hole is $\Delta E_\alpha(T)/2$, $\Sigma'(T)$ of the $3z^2$-r^2 electron should be $\Delta E_A(T) - \Delta E_\alpha(T)/2$. In addition, $\Sigma'(T)$ of the $3z^2$-r^2 electron should be equivalent to $\Delta E_B(T)$ because $\Sigma'(T)$ of the $J_{\rm eff} = 3/2$ holes is nearly T independent. As shown in Fig. 2(d), the two experimental values are indeed very similar to each other, strongly supporting the validity of the peak assignments and our assumption of orbital-dependent $\Sigma'(T)$'s. In short, we succeeded in extracting the $\Sigma'(T)$ of electrons in the $J_{\rm eff} = 1/2$ [Fig. 2(c)] and $3z^2$-r^2 orbitals [Fig. 2(d)]. The T-dependent energies of the $J_{\rm eff} = 1/2$ and $3z^2$-r^2 electrons in the interacting regime are described schematically by the dashed lines in Fig. 1(b).

The obtained $\Sigma'(T)$'s can be well explained in terms of e-ph interactions. In the Fröhlich polaron model [21,22], $\Sigma'(T)$ decreases the electron energy due to the coupling with a single LO phonon. The $\Sigma'(T)$'s of electrons in the optical transition will decrease accordingly by $\hbar\omega_{LO}\alpha_p(n+1)$, where $\hbar\omega_{LO}$ is the LO phonon energy, α_p is the e-ph coupling constant, and n is the Bose-Einstein occupation number, $n = 1/[\exp(\hbar\omega_{LO}/k_B T) - 1]$. Using this model, we can reproduce the $\Sigma'(T)$'s of the electrons very well. The black thick lines in Figs. 2(c) and 2(d) show the best fitting results for the $\Sigma'(T)$ of the $J_{\rm eff} = 1/2$ electron [$\Delta E_\alpha(T)/2$, $\Delta E_\beta(T)$, and $\Delta E_\gamma(T)$] and the $3z^2$-r^2 electron [$\Delta E_A(T) - \Delta E_\alpha(T)/2$ and $\Delta E_B(T)$]. We got $\hbar\omega_{LO} = 54 \pm 4$ meV and $\alpha_p = 4.4 \pm 0.4$ for the $J_{\rm eff} = 1/2$ electron, and $\hbar\omega_{LO} = 32 \pm 5$ meV and $\alpha_p = 5.5 \pm 0.6$ for the $3z^2$-r^2 electron. The values of α_p's are similar to those in a prototypical superconductor La_2CuO_4 ($\alpha_p \sim 5.3$) [28], implying that a strong e-ph interaction indeed exists in Sr_2IrO_4.

These two fits suggest a two-mode e-ph coupling. Namely, the polaron formation occurs in an orbital-dependent way. As described above, we should use distinct phonon energies for
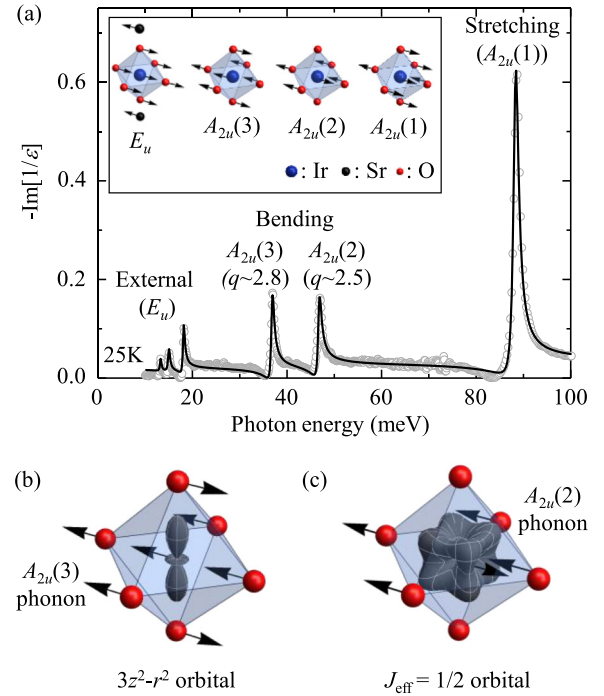
FIG. 3. (Color online) (a) $-\,{\rm Im}(1/\varepsilon)$ of Sr_2IrO_4 taken at 25 K. The six sharp peaks correspond to LO phonon modes. Each phonon mode is illustrated in the inset. Schematics of the formation of polarons in the cases of (b) $3z^2$-r^2 electrons and (c) $J_{\rm eff} = 1/2$ electrons.

the $J_{\rm eff} = 1/2$ and $3z^2$-r^2 electrons. To clarify this point, we plotted the fitting lines with 54 meV (red thin line) and 32 meV (black thick line) phonon energies together in Fig. 2(d). To compare the T dependences of the two lines, we used arbitrary α_p values to match the $T = 400$ K experimental data for both lines. In Fig. 2(d), it is clearly shown that the $\Sigma'(T)$ of the $3z^2$-r^2 electron is very different from the fitting line with 54 meV: Compared to the experimental data, the fitting line starts to decrease at a higher temperature with a steeper slope. Therefore, our results clearly show that the $J_{\rm eff} = 1/2$ electrons effectively couple with the 54 meV phonon mode while the $3z^2$-r^2 electrons couple with the 32 meV phonon mode.

To identify the two phonons that couple with the $J_{\rm eff} = 1/2$ and $3z^2$-r^2 electrons, we investigated the energy-loss spectra. Figure 3(a) shows the energy-loss function of Sr_2IrO_4 taken at $T = 25$ K. The sharp resonances correspond to infrared-active LO phonon modes, while the small backgrounds originate from the tail of peak α. Such an incoherent spectral weight at low energies is also expected in recent theoretic calculations [29]. Below 100 meV, there are three groups of LO phonon modes [30–32]. Three peaks below 20 meV correspond to external phonon modes (E_u), and the highest-energy peak at 89 meV [$A_{2u}(1)$] corresponds to a stretching mode. The two peaks at 37 and 47 meV correspond to out-of-plane [$A_{2u}(3)$] and in-plane [$A_{2u}(2)$] bending modes, respectively. We assigned the symmetries of phonons following the description of a previous work [33]. The atomic displacements for these phonon modes are illustrated in the inset of Fig. 3(a).

The asymmetric line shapes of LO phonons in Fig. 3(a) indicate the existence of large e-ph interactions in Sr_2IrO_4. When discrete excitations, including phonons and core-level excitations, interact with some continuum, they have asymmetric Fano line shapes [34]. The solid lines in Fig. 3(a) are the fitting results using a Fano scattering cross section given by

$$A \frac{(q\Gamma_{ph}/2 + E - E_{ph})^2}{(\Gamma_{ph}/2)^2 + (E - E_{ph})^2}, \qquad (1)$$

where A, Γ_{ph}, E_{ph}, and q are the scaling factor, phonon linewidth, phonon energy, and Fano parameter, respectively. The degree of asymmetry of the phonon mode is quantified by the inverse of q. The q values obtained for the two bending modes were ~ 2.5 [$A_{2u}(2)$] and ~ 2.8 [$A_{2u}(3)$]. The values are similar to those in manganites [35] or cuprates [36] ($q \sim 3$), indicating that LO phonons and electronic excitations in Sr_2IrO_4 strongly couple with each other.

We notice that the fitting parameter $\hbar\omega_{LO}$ for $3z^2$-r^2 electrons (32 ± 5 meV) in our Fröhlich polaron analysis is very close to the measured energy of the $A_{2u}(3)$ mode (37 meV), while that for $J_{eff} = 1/2$ electrons (54 ± 4 meV) is closer to the measured energy of the $A_{2u}(2)$ mode (47 meV). This indicates that the $A_{2u}(3)$ [$A_{2u}(2)$] mode is a plausible candidate for coupling with $3z^2$-r^2 ($J_{eff} = 1/2$) electrons. Considering the orbital symmetry and phonon modes, we can qualitatively explain why $3z^2$-r^2 ($J_{eff} = 1/2$) electrons mainly couple with the $A_{2u}(3)$ [$A_{2u}(2)$] mode. In Figs. 3(b) and 3(c), the orbital and phonon oscillations in an IrO_6 octahedron are schematically described for both cases of the $A_{2u}(3)$-($3z^2$-r^2) and $A_{2u}(2)$-($J_{eff} = 1/2$) polarons.

As shown in Fig. 3(b), the electron density of the $3z^2$-r^2 orbital is concentrated along the z axis. Thus, the movement of apical oxygen is very important to determine the self-energy of $3z^2$-r^2 electrons. The inset of Fig. 3(a) shows that apical oxygen ions move opposite to Ir only in the $A_{2u}(3)$ mode. Therefore, we can easily guess that $3z^2$-r^2 electrons will strongly couple with the $A_{2u}(3)$ mode. This simple argument is consistent with our observations. In contrast, the wave function of $J_{eff} = 1/2$ electrons has a cubic symmetry, as shown in Fig. 3(c). Therefore, the movement of every O ion equally contributes to their self-energy. The inset of Fig. 3(a) shows that only two O ions move opposite to Ir in the $A_{2u}(1)$ and

$A_{2u}(3)$ modes, while four O ions move opposite to Ir in the $A_{2u}(2)$ mode. Thus, it is natural that $J_{eff} = 1/2$ electrons mainly couple with the $A_{2u}(2)$ mode. Although these symmetry-based assessments are not complete but necessitate further detailed evaluations of the e-ph coupling matrix elements, they would provide proper insights on the selectivity of the majority polarons.

In view of the results so far achieved, we propose that orbital-dependent polaron formation occurs in Sr_2IrO_4. Namely, $J_{eff} = 1/2$ electrons and holes mainly couple with the $A_{2u}(2)$ mode, while $3z^2$-r^2 electrons couple with the $A_{2u}(3)$ mode [37]. For $J_{eff} = 3/2$ holes, their T-independent self-energy implies that they do not seem to couple with any phonons. Because the e-ph interaction is generally facilitated by a large effective mass [21], we think that the dispersive nature of the $J_{eff} = 3/2$ orbitals might suppress the e-ph interaction. Such an orbital dependence in the e-ph interaction seems to be natural, but few reports that resolve this interaction have been presented so far [38]. In TMOs, the orbital-dependent e-ph interaction should be enhanced because electrons are strongly localized and retain atomiclike orbitals. Therefore, we believe that our results provide fundamental information about the e-ph interaction in TMOs, and can be applied to a variety of different systems.

In summary, we provided orbital-resolved information on the e-ph interaction in Sr_2IrO_4. The overall T dependence in the optical spectra is well explained in terms of the Fröhlich polaron model. We showed promising evidence that the e-ph interaction in Sr_2IrO_4 varies depending on the orbital symmetries. Considering the symmetries of the orbital and phonons, we proposed plausible candidates of phonons that mainly couple with $J_{eff} = 1/2$ and $3z^2$-r^2 electrons. The concept of orbital dependence in e-ph interactions will be essential for understanding the low-energy physics in various TMOs.

[1] B. J. Kim, H. Jin, S. J. Moon, J.-Y. Kim, B.-G. Park, C. S. Leem, J. Yu, T. W. Noh, C. Kim, S.-J. Oh, J.-H. Park, V. Durairaj, G. Cao, and E. Rotenberg, Phys. Rev. Lett. **101**, 076402 (2008).

[2] B. J. Kim, H. Ohsumi, T. Komesu, S. Sakai, T. Morita, H. Takagi, and T. Arima, Science **323**, 1329 (2009).

[3] S. J. Moon, H. Jin, K. W. Kim, W. S. Choi, Y. S. Lee, J. Yu, G. Cao, A. Sumi, H. Funakubo, C. Bernhard, and T. W. Noh, Phys. Rev. Lett. **101**, 226402 (2008).

[4] A. Shitade, H. Katsura, J. Kuneš, X.-L. Qi, S.-C. Zhang, and N. Nagaosa, Phys. Rev. Lett. **102**, 256403 (2009).

[5] C. H. Kim, H.-S. Kim, H. Jeong, H. Jin, and J. Yu, Phys. Rev. Lett. **108**, 106401 (2012).

[6] H.-S. Kim, C. H. Kim, H. Jeong, H. Jin, and J. Yu, Phys. Rev. B **87**, 165117 (2013).

[7] J. Chaloupka, G. Jackeli, and G. Khaliullin, Phys. Rev. Lett. **105**, 027204 (2010).

[8] Y. Singh, S. Manni, J. Reuther, T. Berlijn, R. Thomale, W. Ku, S. Trebst, and P. Gegenwart, Phys. Rev. Lett. **108**, 127203 (2012).

[9] J. Chaloupka, G. Jackeli, and G. Khaliullin, Phys. Rev. Lett. **110**, 097204 (2013).

[10] G. Cao, T. F. Qi, L. Li, J. Terzic, V. S. Cao, S. J. Yuan, M. Tovar, G. Murthy, and R. K. Kaul, Phys. Rev. B **88**, 220414(R) (2013).

[11] T. Takayama, A. Matsumoto, J. Nuss, A. Yaresko, K. Ishii, M. Yoshida, J. Mizuki, and H. Takagi, arXiv:1311.2885.

[12] G. Zhao, K. Conder, H. Keller, and K. A. Müller, Nature (London) **381**, 676 (1996).

[13] G. Zhao, M. B. Hunt, H. Keller, and K. A. Müller, Nature (London) **385**, 236 (1997).

[14] C. Gadermaier, A. S. Alexandrov, V. V. Kabanov, P. Kusar, T. Mertelj, X. Yao, C. Manzoni, D. Brida, G. Cerullo, and D. Mihailovic, Phys. Rev. Lett. **105**, 257001 (2010).

[15] M. Sentef, A. F. Kemper, B. Moritz, J. K. Freericks, Z.-X. Shen, and T. P. Devereaux, Phys. Rev. X **3**, 041033 (2013).

[16] W. S. Lee, S. Johnston, B. Moritz, J. Lee, M. Yi, K. J. Zhou, T. Schmitt, L. Patthey, V. Strocov, K. Kudo, Y. Koike, J. van den Brink, T. P. Devereaux, and Z. X. Shen, Phys. Rev. Lett. **110**, 265502 (2013).

[17] P. D. C. King, T. Takayama, A. Tamai, E. Rozbicki, S. McKeown Walker, M. Shi, L. Patthey, R. G. Moore, D. Lu, K. M. Shen, H. Takagi, and F. Baumberger, Phys. Rev. B **87**, 241106(R) (2013).

[18] H. J. Park, C. H. Sohn, D. W. Jeong, G. Cao, K. W. Kim, S. J. Moon, H. Jin, D.-Y. Cho, and T. W. Noh, Phys. Rev. B **89**, 155115 (2014).

[19] H. Gretarsson, J. P. Clancy, Y. Singh, P. Gegenwart, J. P. Hill, J. Kim, M. H. Upton, A. H. Said, D. Casa, T. Gog, and Y.-J. Kim, Phys. Rev. B **87**, 220407(R) (2013).

[20] D. Pröpper, A. N. Yaresko, T. I. Larkin, T. N. Stanislavchuk, A. A. Sirenko, T. Takayama, A. Matsumoto, H. Takagi, B. Keimer, and A. V. Boris, Phys. Rev. Lett. **112**, 087401 (2014).

[21] H. Fröhlich, Adv. Phys. **3**, 325 (1954).

[22] H. Y. Fan, Phys. Rev. **82**, 900 (1951).

[23] G. Cao, J. Bolivar, S. McCall, J. E. Crow, and R. P. Guertin, Phys. Rev. B **57**, R11039 (1998).

[24] C. C. Homes, M. Reedyk, D. A. Cradles, and T. Timusk, Appl. Opt. **32**, 2976 (1993).

[25] S. J. Moon, M. W. Kim, K. W. Kim, Y. S. Lee, J.-Y. Kim, J.-H. Park, B. J. Kim, S.-J. Oh, S. Nakatsuji, Y. Maeno, I. Nagai, S. I. Ikeda, G. Cao, and T. W. Noh, Phys. Rev. B **74**, 113104 (2006).

[26] We extracted the energies of d-d transitions from the dips in $d^2\varepsilon_2(\omega)/d\omega^2$ to minimize the fitting errors. According to the Lorentz oscillator model for $\varepsilon_2(\omega)$, the dips in $d^2\varepsilon_2(\omega)/d\omega^2$ correspond to the peaks in $\varepsilon_2(\omega)$.

[27] Q. Huang, J. L. Soubeyroux, O. Chmaissem, I. Natali Sora, A. Santoro, R. J. Cava, J. J. Krajewski, and W. F. Peck, Jr., J. Solid State Chem. **112**, 355 (1994).

[28] J. P. Falck, A. Levy, M. A. Kastner, and R. J. Birgeneau, Phys. Rev. Lett. **69**, 1109 (1992).

[29] H. Zhang, K. Haule, and D. Vanderbilt, Phys. Rev. Lett. **111**, 246402 (2013).

[30] L. Pintschovius, J. M. Bassat, P. Odier, F. Gervais, G. Chevrier, W. Reichardt, and F. Gompf, Phys. Rev. B **40**, 2229 (1989).

[31] S. Tajima, T. Ido, S. Ishibashi, T. Itoh, H. Eisaki, Y. Mizuo, T. Arima, H. Takagi, and S. Uchida, Phys. Rev. B **43**, 10496 (1991).

[32] S. J. Moon, H. Jin, W. S. Choi, J. S. Lee, S. S. A. Seo, J. Yu, G. Cao, T. W. Noh, and Y. S. Lee, Phys. Rev. B **80**, 195110 (2009).

[33] M. F. Cetin, P. Lemmens, V. Gnezdilov, D. Wulferding, D. Menzel, T. Takayama, K. Ohashi, and H. Takagi, Phys. Rev. B **85**, 195148 (2012).

[34] U. Fano, Phys. Rev. **124**, 1866 (1961).

[35] S. Naler, M. Rübhausen, S. Yoon, S. L. Cooper, K. H. Kim, and S. W. Cheong, Phys. Rev. B **65**, 092401 (2002).

[36] S. Lupi, M. Capizzi, P. Calvani, B. Ruzicka, P. Maselli, P. Dore, and A. Paolone, Phys. Rev. B **57**, 1248 (1998).

[37] Here, we did not consider the Raman-active modes. It is because a previous time-resolved spectroscopy showed there are no coherent phonons in the decay process [D. Hsieh, F. Mahmood, D. H. Torchinsky, G. Cao, and N. Gedik, Phys. Rev. B **86**, 035128 (2012)], suggesting that the Raman-active modes might not couple with the electron or hole as strong as the infrared-active modes. Further experiments and theoretical studies are needed to clarify this issue.

[38] Z. Sun, I. Swart, C. Delerue, D. Vanmaekelbergh, and P. Liljeroth, Phys. Rev. Lett. **102**, 196401 (2009).